HETEROCYCLES, Vol. 105, No. 1, 2022, pp. 544 - 555. © 2022 The Japan Institute of Heterocyclic Chemistry
Received, 21st December, 2021, Accepted, 2nd March, 2022, Published online, 8th March, 2022
DOI: 10.3987/COM-21-S(R)9

IMPROVED SYNTHESIS OF NALDEMEDINE TOSYLATE AND CRYSTAL STRUCTURES OF FOUR RELATED SOLID FORMS

Josef Spreitz,[1] Thomas Gelbrich,[2] Sven Nerdinger,[3]* Marijan Stefinovic,[3] and Ulrich J. Griesser [2]*

[1] Aglycon Dr. Spreitz KG, Europapark 1, A-8412 Allerheiligen b. Wildon, Austria; [2] University of Innsbruck, Institute of Pharmacy, Innrain 52c, 6020 Innsbruck, Austria; [3] Sandoz GmbH, Biochemiestrasse 10, 6250 Kundl, Austria. E-mail: sven.nerdinger@sandoz.com, ulrich.griesser@uibk.ac.at

This paper is dedicated to Professor Somsak Ruchirawat on the occasion of his 80th birthday.

Abstract – The production of drug substances requires a robust and scalable process capable of delivering the active pharmaceutical ingredient (API) in excellent chemical and polymorphic purity. With this goal in mind we have developed an improved procedure for the preparation of naldemedine tosylate, which crystallizes directly from the reaction mixture as pure polymorph form II. Solid state studies revealed a series of additional new physical forms whose crystal structure have been determined by single-crystal X-ray diffraction.

S-297995, better known as naldemedine (**1**), is a modified analogue of Naltrexone[1] developed by Shionogi. It is a potent opioid receptor-antagonizing morphinan which has been investigated as an oral treatment for opioid-induced constipation. Naldemedine was approved in the USA and Japan in 2017 and in the EU in 2019. It is marketed under the trade name *Symproic* in the US and as Rizmoic in the European Union.

Two syntheses of naldemedine (**1**) have been reported so far. The first route was reported by Inagaki *et al.*,[2] as shown in Scheme 1. The synthesis starts with compound (**2**), a benzyl protected oxymorphone derivative, which is carboxyethylated alpha to the keto group to afford ester (**3**). Benzyl protection using benzyl alcohol and 1,1'-(azodicarbonyl)dipiperidine (ADDP) affords the doubly protected ester (**5**), which is hydrolysed to the corresponding acid (**6**). Activation of the carboxyl group and subsequent reductive

debenzylation of both hydroxy groups affords naldemedine (**1**) as free base in 23% yield over five linear steps.

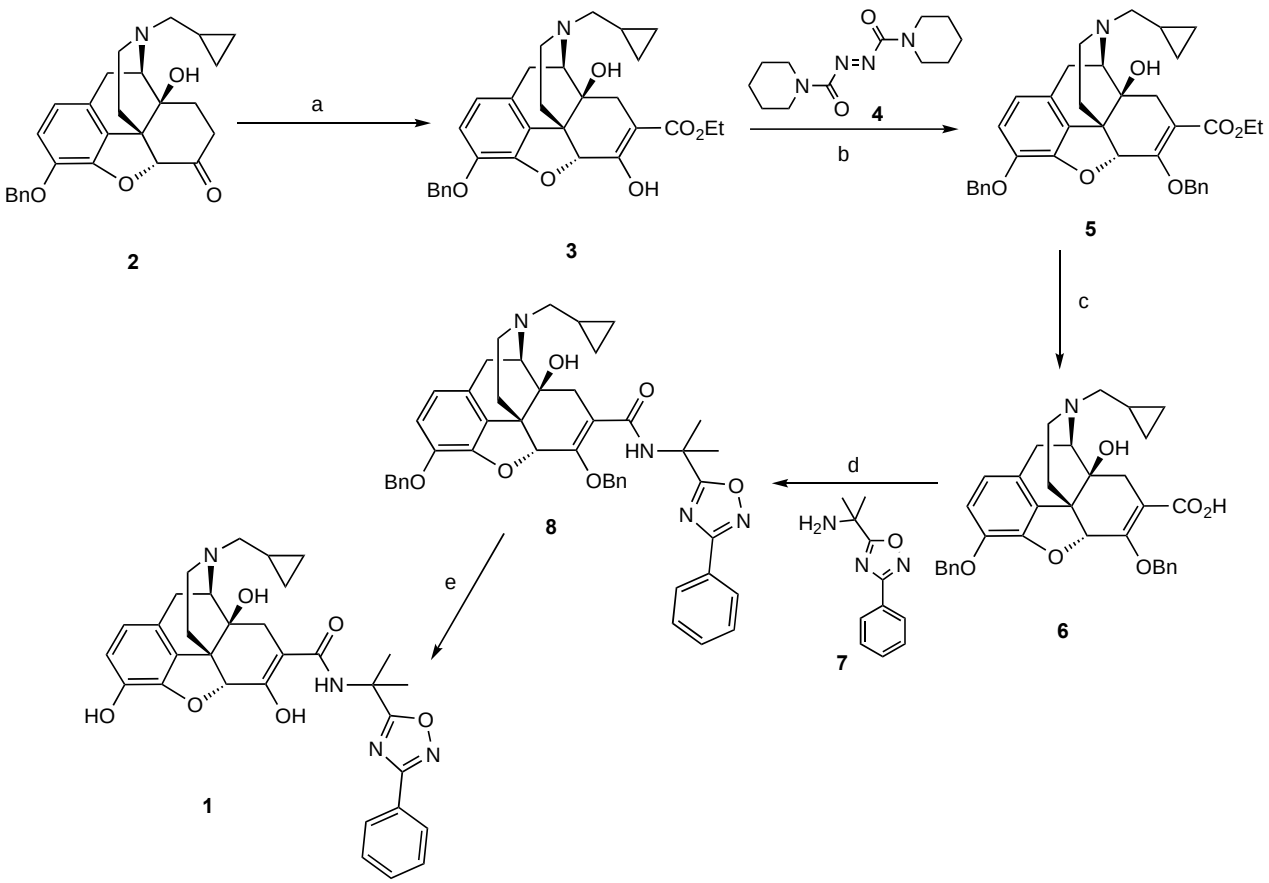

Scheme 1. First synthesis of naldemedine (**1**): (a) NaH/$CO(OEt)_2$, 100 °C, 49%; (b) **4**, $P(^nBu)_3$, BnOH, THF, –10 °C, 98%; (c) i) KOH, 50 °C MeOH/dioxane; ii) HCl, 77%; (d) **7**, EDC, HOBt, THF, rt, 73%; (e) $Pd(OH)_2/H_2$, MeOH, rt, 86%.

Another route to naldemedine (**1**) and its tosylate salt (**15**) were reported by Tamura *et al.*[3] and is shown in Scheme 2. This route is based on an unusual copper(II)-mediated formation of carbamate **14** via condensation of isocyanate **11** with alcohol **13**. Heating **14** with KOH and *i*-PrOH to 80 °C induces the migration of the oxadiazolyl moiety to the C-7 position to give naldemedine free base (**1**) which is then converted into its toslyte salt (**15**) via salt formation. The overall yield of this four step process to naldemedine tosylate (**15**) is 69%. Whilst the conditions given by Tamura *et al.*[3] are suitable for small scale synthesis, they are not workable on multigram scale.[4] On multigram scale the synthesis produces a very low yield of **1**, in part due to poor conversions in step d). A significant part of the yield loss in this step was attributable to the precipitation of copper salts. The finely divided suspension produced during the bi-phasic reaction made the aqueous-organic phase separation impossible. To overcome the issue of poor phase separation & isolation of step d), we investigated the use of a different Lewis acid catalyst, in particular, one where a fine precipitate would be avoided during phase separation & isolation and one

mild enough to leave the acetyl group intact.[5] One such reagent is dibutyltin dilaurate (DBTL) whose use has only been described in the polymer industry and only a few examples are known to the best of our knowledge.[6-8] Replacement of $CuCl_2$ by DBTL (0.07 equiv.) gave **14** in 94% yield. In contrast to $CuCl_2$, DBTL produced a homogeneous reaction mixture which produced a filterable solid upon addition of *n*-hexane compared to the original procedure where only suspension was obtained. Initial attempts to induce the key rearrangement from **14** to naldemedine free base (the migration of the oxadiazolyl moiety to the C-7 position) were not successful. We could only isolate product **16** whose structure was unambiguously confirmed by single crystal structure analysis (see below). After some experimentation we found that simply extending the reaction time to 16 h at 85 °C was the best way to achieve a reasonable yield of naldemedine (**1**). The modified synthesis is shown in Scheme 2.

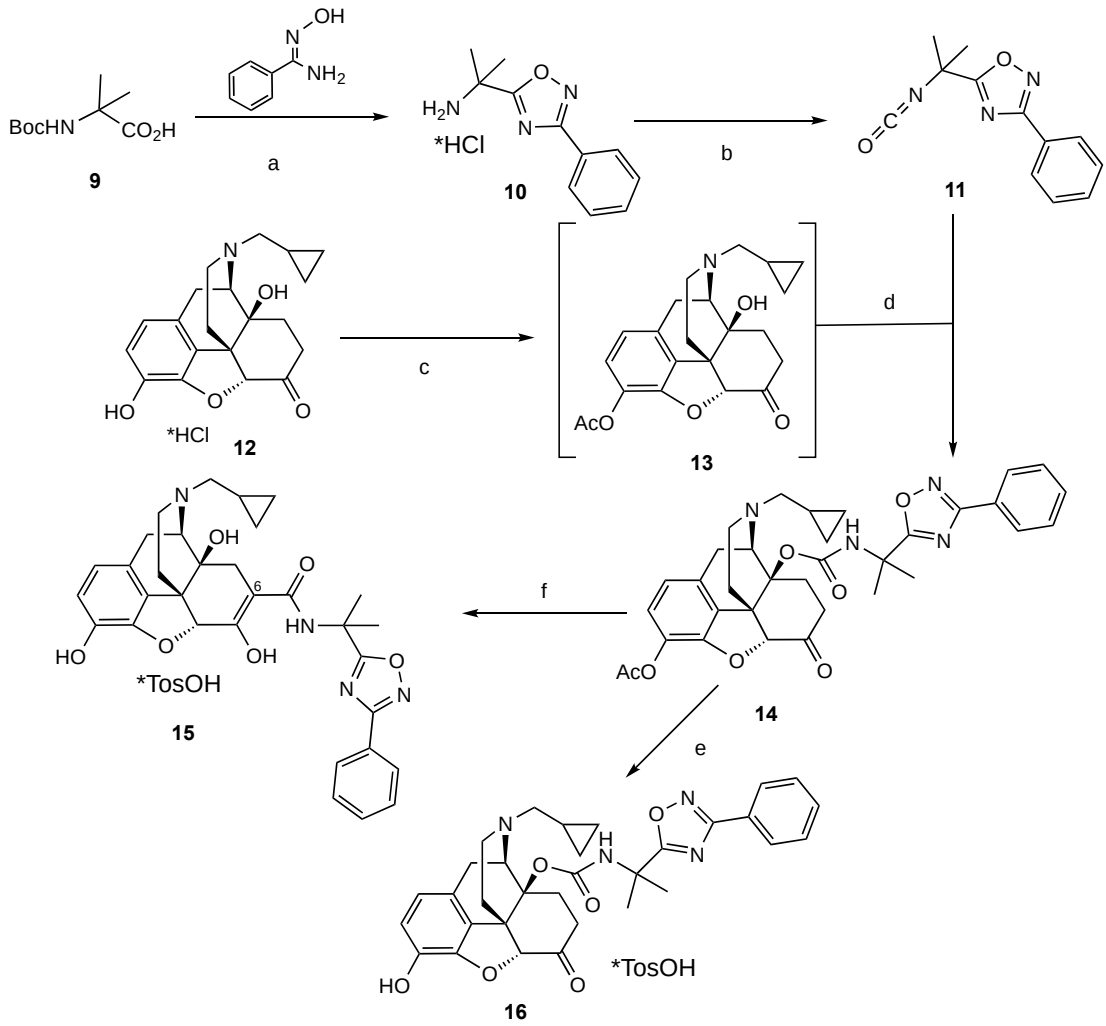

Scheme 2. Preparation of naldemedine tosylate (**15**) and improved process: (a) $^{i}Pr_2NEt$, $^{i}BuCOCl$, $^{n}PrOAc$, 0 °C->heat, 93%; (b) i) MeOCOCl, toluene, heat; ii) BCl_3, toluene, NEt_3, 50 °C, 93% (overall); (c) Ac_2O, NEt_3, EtOAc, 40 °C, 94% (recryst.); (d) **11**, DBTL, EtOAc, rt, 94%; (e) i) KOH, $^{i}PrOH$, 80 °C, 5 h, 69%; ii) TsOH, MeOH; iii) MeCN, rt, 48%; (f) i) KOH, $^{i}PrOH$, 85 °C, 16 h, 69%; ii) TsOH, MeOH, heat, 89%.

Both the unsolvated form of **15** and the corresponding MeOH (**15·MeOH**) crystallise in the space group $P2_12_12_1$ with one crystallographically independent formula unit (Table 1). Our structure determination has confirmed the configuration of the chiral centers as C20(S), C21(R), C25(S) and C26(R). The structure of naldemedinium structure of **15** is shown in Figure 1a. The cation possesses five potential donor (*D*) sites, i.e. namely three OH groups (O36, O37, O38), the secondary amino function (N13) and the aminium group (N33). It displays intramolecular O37–H···O15 and N33–H···O36 bonds. In addition, one-point H-bond connections are formed to three different anions *via D*–H···O interactions (D: N33, O36, O37), resulting in an H-bonded framework structure. An overlay of the naldemedinium ions of **15** and **15·MeOH** confirms that essentially the same cation geometry is present in both structures [root-mean-square deviation ($rmsd_1$) of 0.1508 Å for all non-H atomic positions,[10] see Figure S1a of the Supporting Information]. Moreover, **15** and **15·MeOH** are isostructural with regard to the 3D packing arrangement of naldemedinium units, and the corresponding *XPac* comparison[11] resulted in a dissimilarity index[12] *x* of 4.0 (for details, see Figure S2 of the Supporting Information). It is therefore not surprising that the complete set of classical intramolecular and intermolecular H-bond interactions previously discussed for **15** is also found in the analogous MeOH solvate. Interestingly, the H-bonded framework of **15** contains solvent-accessible voids[9] of 49 $Å^3$. In the isostructural **15·MeOH** solvate, these same sites are occupied by solvent (*s*) molecules (Figure 2b, c), with the latter participating in additional H-bonds, N33–H···O(s) and (*s*)O–H···$O37^{iii}$. The first of these interactions involves the N13 amino group, which in **15** is not engaged in hydrogen bonding. Thus, the solvent molecule serves as an additional H-bonded bridge between neighboring cation units, which is accompanied by an increase in intermolecular N13···$O37^{iii}$ separation of 0.39 Å. The incorporation of MeOH in the H-bonded framework results in a volume increase per formula unit due of 14.6 $Å^3$ and in a significantly higher packing coefficient (0.681 *vs.* 0.668).

Two phases of **16** were investigated, namely an acetonitrile solvate (**16·ACN**) and an acetone solvate hydrate (**16·ACE·H_2O**), both crystallizing in the space group $P2_1$ with one formula unit in the asymmetric unit and similar unit cell parameters (Table 1). The cation (Figure 1b) displays three potential donor groups for hydrogen bonds, namely the OH group (O37), the secondary amino function (N13) and the aminium group (N33). In the case of **16·ACN**, the cation forms N13–H···$O3A^i$ and N33–H···$O3A^i$ bonds to the same O atom of an anion. It is also connected to second anion *via* an O37–H···O1A interaction (Figure 3b). The ACN molecule does not participate in hydrogen bonding. These intermolecular interactions give rise to a dense H-bonded tape structure, which propagates parallel to the *b* axis. As shown in Figure 3a, there are significant differences between the cation geometries found in **16·ACN** and **16·ACE·H_2O** (except for the rigid morphinan skeleton; $rmsd_1$ = 0.4749 Å; see Figure S1b of the Supporting Information). A corresponding *XPac* analysis revealed that although the solvates

16·ACN and **16·ACE·H$_2$O** share the same fundamental 3D packing of cations, the incorporation of ACN *vs.* ACE and water requires significant geometrical adjustments, as indicated by an elevated dissimilarity index (x = 11.0). In addition to the conformational differences discussed above (Figure 3a), **16·ACN** and **16·ACE·H$_2$O** also show distinct hydrogen bond patterns. The N33–H···O3A interaction is present in both crystals. In **16·ACN**, the amino group of the cation is H-bonded to the sulfonic acid group of the anion. However, in **16·ACE·H$_2$O** the same group is linked to the OH group of a neighboring cation, N13–H···O37^{ii} (Figure 3b, c) and an O37–H···O1W bond is formed with the water molecule. The latter also donates an O1W–H···O38 bond back to the same cation moiety and additionally an O1W–H···O2A^{i} bond to an anion (Figure 3c). The water molecule serves therefore as an H-bonded bridge between two cations and one anion. The ACE molecule does not participate in any classical H-bond interactions. Altogether, each cation is H-bonded to two other cations, one anion and one water molecule, yielding a hydrogen-bonded tape structure parallel to the *b* axis. The increase in volume due to the replacement of ACN with ACE plus H$_2$O is 27.4 Å per formula unit and leaves the packing coefficient almost unchanged (0.672 *vs.* 0.669).

Table 1. Crystallographic parameters and refinement details

Compound	**15**	**15·MeOH**	**16·ACN**	**16·ACE·H$_2$O**
Moiety formula	$C_{32}H_{35}N_4O_6^+ \cdot C_7H_7O_3S^-$	$C_{32}H_{35}N_4O_6^+ \cdot C_7H_7O_3S^- \cdot CH_4O$	$C_{32}H_{35}N_4O_6^+ \cdot C_7H_7O_3S^- \cdot C_2H_3N$	$C_{32}H_{35}N_4O_6^+ \cdot C_7H_7O_3S^- \cdot C_3H_6O \cdot H_2O$
Empirical formula	$C_{39}H_{42}N_4O_9S$	$C_{40}H_{46}N_4O_{10}S$	$C_{41}H_{45}N_5O_9S$	$C_{42}H_{50}N_4O_{11}S$
Formula weight	742.82	774.87	783.88	818.92
Temperature [K]	173	173	173	173
Wavelength [Å]	0.71073	0.71073	0.71073	1.54184
Crystal system	Orthorhombic	Orthorhombic	Monoclinic	Monoclinic
Space group	$P2_12_12_1$	$P2_12_12_1$	$P2_1$	$P2_1$
a [Å]	22.5969(9)	22.5650(14)	12.9257(14)	13.6794(2)
b [Å]	13.2354(7)	13.1928(9)	9.3569(8)	9.50568(19)
c [Å]	12.4597(8)	12.7145(10)	16.2822(19)	15.9156(3)
β [°]			95.891(10)	92.0561(15)
V [Å^3]	3726.4(3)	3785.0(5)	1958.8(4)	2068.21(6)
Z / Z'	4 / 1	4 / 1	2 / 1	2 / 1
d_{calc} [g·cm^{-3}]	1.324	1.360	1.329	1.315
Crystal size [mm^3]	0.25× 0.20 × 0.10	0.40 × 0.40 × 0.25	0.20 × 0.20 × 0.10	0.30 × 0.20 × 0.05
θ range [°]	3.3 – 25.4	3.5 – 26.4	3.5 – 25.4°	4.2 – 67.5
Reflections coll. / R_{int}	12922 / 0.0422	15688 / 0.0292	16561 / 0.0512	26064 / 0.0404
Data / restraints / parameters	6788 / 5 / 503	7496 / 6 / 526	7169 / 57 / 581	7392 / 6 / 587
Goodness-of-fit on F^2	1.004	1.032	1.013	1.055
$R1$ [$I > 2\sigma(I)$]	0.0521	0.0362	0.0604	0.0347
$wR2$ (all data)	0.1114	0.0804	0.1543	0.0905
Absolute structure parameter	0.08(7)	–0.02(3)	0.04(8)	–0.002(7)
Largest diff. peak / hole [e·Å^{-3}]	0.331 / –0.220	0.332 / –0.275	0.245 / –0.249	0.197 / –0.281
CCDC no.	2010655	2010653	2010654	2010652

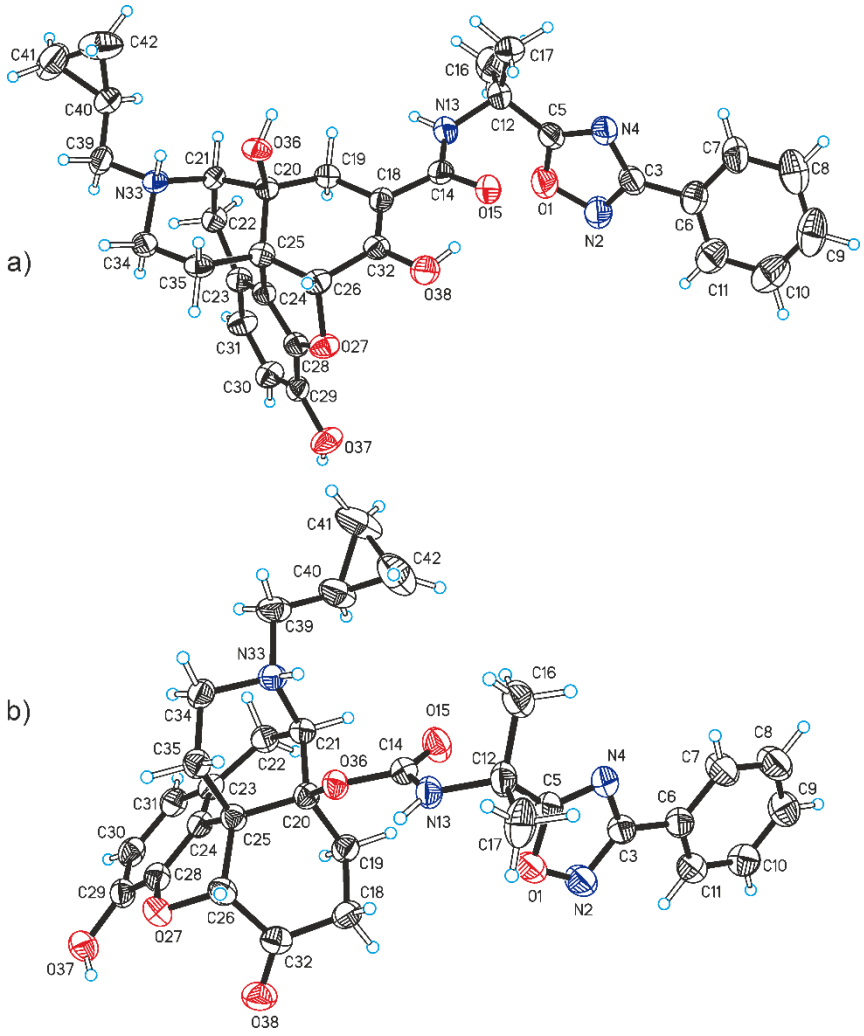

Figure 1. Molecular structure of the naldemedinium ion in the crystal structures of **15 (a)** and **16·ACE·H$_2$O (b)** (non-H atoms are represented as thermal ellipsoids drawn at the 50% probability level, and H atoms are represented as spheres of random size).

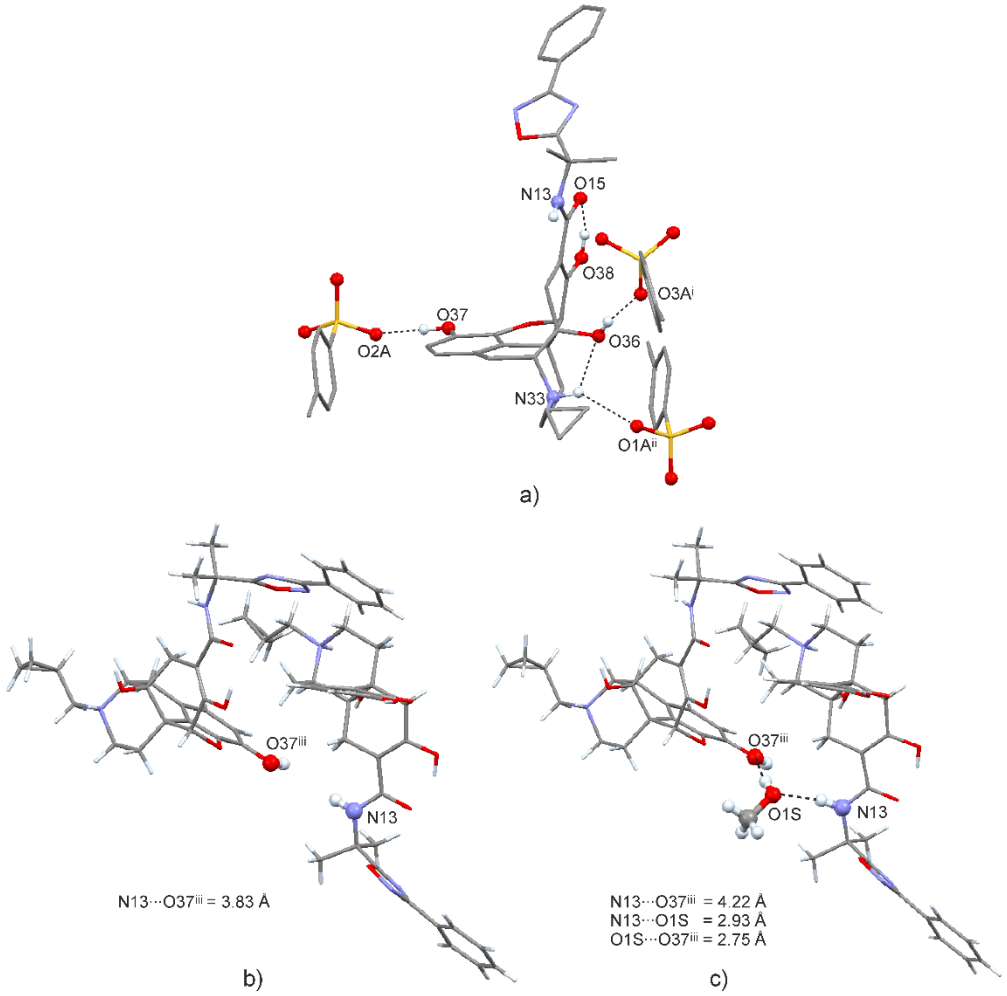

Figure 2. a) Fragment of the crystal structure of **15** showing a central naldemedinium ion which donates the hydrogen bonds for one N–H···O and two O–H···O interactions to three tosylate ions. Note that the N13–H group is not engaged in classical H-bonding. **b)** Supramolecular arrangement showing the closest intermolecular contact of the N13–H group in **15** and **c)** the analogous fragment in **15·MeOH** with MeOH serving as an H-bonded bridge *via* N13–H···O1S–H···O37^{iii}. Symmetry codes: (i) -x+3/2, -y+1, z-1/2 (ii) x+1/2, -y+3/2, -z+1 (iii) -x+3/2, -y+1, z-1/2.

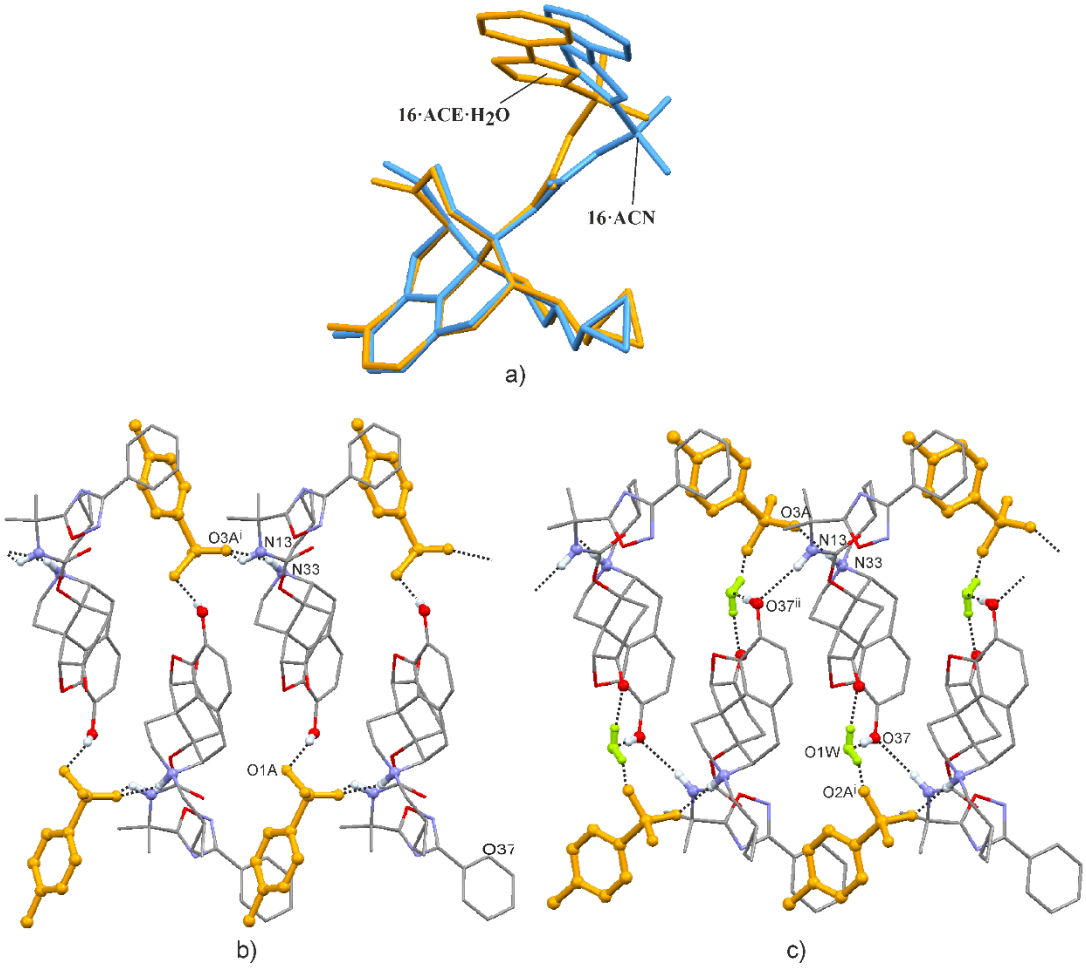

Figure 3. a) Least-squares fit of the morphinan skeletons present in two solvates of **16**. H-bonded tape structures of **b) 16·ACN** and **c) 16·ACE·H2O**, both viewed along [-101] (orange: tosylate ions; green: water molecules; ACN and ACE molecules and H atoms not involved in hydrogen bonding omitted for clarity). Symmetry codes: (i) -x+1,y-1/2,-z+1; (ii) 2 -x+1,y+1/2,-z+1].

In summary, we have developed an improved process to naldemedine tosylate which enabled the supply of ca. 30 g for subsequent solid state screening activities. We have determined the single crystal structures of pairs of closely related solid forms of two compounds associated with this preparation.

EXPERIMENTAL

Reagents and solvents were purchased from Sigma-Aldrich. NMR spectra were recorded with a Bruker Avance DPX 300 spectrometer. IR spectra were obtained with a Bruker ALPHA Platinum FT-ATR instrument. High resolution mass spectra were measured with a Finnigan MAT 95 mass spectrometer.

Intensity data were recorded at 173 K, using a Nonius Kappa CCD Gemini Ultra diffractometer and Mo$K\alpha$ radiation (λ = 0.71073 Å) or Cu$K\alpha$ radiation (λ = 1.54184 Å) in the case of **16·ACE·H2O**. The

data were corrected for absorption effects using *SADABS*.[13] The crystal structures were solved by Direct Methods with *SHELXT*[14] and refined by full-matrix least-squares techniques using *SHELXL*.[15] The positions of H atoms were identified from difference maps, those bonded to C atoms were included in the refinement using a riding model with U_{iso} set to 1.2 or 1.5U_{eq} of the parent C atom. H atoms bonded to O or N atoms were refined using distance restraints [O–H = 0.84(1) Å, N–H = 0.88(1) Å] and their temperature factors were refined freely. In, **16·ACN** both the terminal cyclopropylmethyl group of the cation and the sulfonic acid group of the anion are disordered over two orientations with 50% occupancy. Distance restraints for chemically equivalent 1,2- and 1,3-distances were applied in the refinement of the disorder components. Geometrical parameters of hydrogen bonds are listed in section 1 of the Supporting Information. CCDC Accession Codes 2010652-5 contain the supplementary crystallographic data for this paper, all of which can be obtained free of charge at www.ccdc.cam.ac.uk/data_request/cif, by emailing data_request@ccdc.cam.ac.uk, or contacting The Cambridge Crystallographic Data Centre, 12 Union Road, Cambridge CB2 1EZ, UK; fax: +44 1223 336033.

Comparison of crystal structures

The program *XPac*[14] was used for the comparison of cation packing arrangements. For each structure, an initial set comprising all 42 non-H atomic positions was used to calculate intermolecular geometrical parameters. Pairwise comparisons between crystal structures were carried out, and standard cut-off parameters were applied to identify cases of packing similarity. For occurrences of packing similarity, a dissimilarity index *x* was calculated in the previously described manner.[15] For details, see section 3 of the Supporting Information.

(4*R*,4a*S*,7a*R*,12b*S*)-3-(Cyclopropylmethyl)-9-hydroxy-7-oxo-1,2,3,4,5,6,7,7a-octahydro-4a*H*-4,12-methanobenzofuro[3,2-*e*]isoquinolin-4a-yl(2-(3-phenyl-1,2,4-oxadiazol-5-yl)propan-2-yl)carbamate 4-methylbenzenesulfonic acid (16)

O-Acetylnaltrexone (**13**) (27.0 g, 70.4 mmol) were dissolved in EtOAc (200 mL) and a solution of 2-(3-phenyl-1,2,4-oxadiazol-5-yl)propan-2-yl isocyanate (**12**) (25.0 g, 110 mmol) in EtOAc (200 mL) was added. Then dibutyltin dilaurate (3.00 g, 4.75 mmol) was added and the mixture was stirred for 24 h at room temperature. To the resulting suspension *n*-hexane (400 mL), stirred for 60 min at rt followed by filtration to yield 40.0 g of an ochre solid. The obtained compound (**14**) was used at the next step without purification.

Compound (**14**) (42.0 g, 68.6 mmol) was suspended in *i*-PrOH (150 mL) before a 2M aqueous solution of KOH (180 mL) was slowly added by means of a dropping funnel under stirring. The resulting suspension was heated and stirred at 80 °C for 5 h. To the resulting suspension water (200 mL) was added and the solution was neutralized with diluted hydrochloric acid. The mixture was extracted with EtOAc (250 mL),

dried over magnesium sulfate. The solvent was removed under reduced pressure and the residue was dissolved CH_2Cl_2 (100 mL). After cooling to 4 °C, the solid was filtered, washed with a small amount of cold CH_2Cl_2, to yield 27.0 g (69%) of an off-white solid after drying.

The residue (20.0 g, 35.0 mmol) was dissolved in MeOH (144 mL) by heating to 50 °C before a solution of *p*-toluenesulfonic acid (8.00 g, 42.1 mmol) in MeOH (80 mL) was slowly added by means of a dropping funnel under stirring. The resulting light brown solution was heated to reflux for 30 min and then concentrated to half of its volume through removal of MeOH by distillation. After cooling to rt the mixture was allowed to stand overnight at 25 °C. The solid was filtered, washed with a little cold MeCN to yield 12.5 g (48%) of an ochre solid after drying. Single crystals were obtained by diffusion of Et_2O into a methanolic solution of (**14**) at 4 °C, Mp 118 – 121 °C (decomp.) ^{1}H-NMR (300 MHz, DMSO-d_6) δ 0.47 (4H, m), 0.95 (1H, m), 1.50-1.57 (1H, m), 1.67 (4H, s), 1.84 (3H, s), 2.23 (1H, m), 2.29 (3H, s), 2.58-2.65 (2H, m), 2.82-2.92 (2H, m), 3.01-3.09 (1H, m), 3.14-3.18 (1H, m), 3.35-3.47 (1H, m), 4.85-4.87 (1H, m), 5.09 (1H, d, *J* = 8.1 Hz), 6.64 (1H, d, *J* = 7.8 Hz), 6.73 (1H, d, *J* = 7.8 Hz), 7.12 (2H, d, *J* = 8.1 Hz), 7.49 (2H, d, *J* = 8.1 Hz), 7.53-7.761 (3H, m), 7.95 (1H, d, *J* = 7.8 Hz), 8.74 (1H, s), 8.87 (1H, s broad), 9.57 (1H, s broad ^{13}C-NMR (75 MHz, DMSO-d_6) δ 206.41, 183.37, 167.66, 153.60, 145.45, 143.46, 140.31, 138.00, 131.75, 129.42, 128.25, 127.04 , 127.01, 126.21, 125.61, 120.66, 120.37, 118.53, 88.13, 79.89, 57.35, 56.98, 51.98, 48.54, 46.05, 34.66, 27.36, 27.23, 25.85, 24.85, 23.24, 20.89, 5.41 ppm.

[(4*R*,4a*S*,7a*R*,12b*S*)-3-(Cyclopropylmethyl)-4a,9-dihydroxy-7-oxo-2,4,5,6,7a,13-hexahydro-1*H*-4,12-methanobenzofuro[3,2-*e*]isoquinolin-9-yl]-*N*-2-(3-phenyl-1,2,4-oxadiazol-5-yl)propan-2-ylcarbamate 4-methylbenzenesulfonic acid (15)

O-Acetylnaltrexone (**13**) (27.0 g, 70.4 mmol) were dissolved in EtOAc (200 mL) and a solution of 2-(3-phenyl-1,2,4-oxadiazol-5-yl)propan-2-yl isocyanate (**12**) (25.0 g, 110 mmol) in EtOAc (200 mL) was added. Then dibutyltin dilaurate (3.00 g, 4.75 mmol) was added and the mixture was stirred for 24 h at room temperature. The resulting suspension was diluted with, *n*-hexane (400 mL) and stirred for 60 min at rt. Filtration afforded 40.0 g of an ochre solid. The obtained compound (**14**) was used at the next step without purification.

Compound (**14**) (42.0 g, 68.6 mmol) was suspended in *i*-PrOH (150 mL) before a 2M aqueous solution of KOH (180 mL) was slowly added by means of a dropping funnel under stirring. The resulting suspension was heated and stirred at 85 °C for 16 h. To the resulting suspension water (200 mL) was added and the solution was neutralized with diluted hydrochloric acid. The mixture was extracted with EtOAc (250 mL), dried over magnesium sulfate. The solvent was removed under reduced pressure and the residue was dissolved in CH_2Cl_2 (100 mL). After cooling to 4 °C, the solid was filtered, washed with a small amount

of cold CH_2Cl_2, to yield 27.0 g (69%) of an off-white solid after drying. The residue (25.0 g, 43.8 mmol) was dissolved in MeOH (180 mL) by heating to 50 °C before a solution of *p*-toluenesulfonic acid (10.0 g, 52.6 mmol) in MeOH (100 mL) was slowly added by means of a dropping funnel under stirring. The resulting light brown solution was heated to reflux for 30 min and then concentrated to half of its volume through removal of MeOH by distillation. After cooling to rt the mixture was allowed to stand overnight at 25 °C. The solid was filtered, washed with a little cold MeCN to yield 28.9 g (89%) of an ochre solid after drying after combining the two crops.

The NMR data were in agreement with known literature or patent data.[1] ^{1}H-NMR (DMSO-d_6) δ 0.29-0.37 (m, 1H), 0.38-0.52 (m, 2H), 0.53-0.64 (m, 1H), 0.86-1.01 (m, 1H), 1.55 (ddd, *J* = 3.8, 15 Hz, 1H), 1.67 (s, 3H), 1.84 (s, 3H), 2.21-2.31 (m, 1H), 2.28 (s, 3H), 2.46-2.55 (m, 1H), 2.56-2.72 (m, 2H), 2.82-3.00 (m, 2H), 3.06 (dd, *J* = 6.2, 20 Hz, 1H), 3.12-3.22 (m, 1H), 3.33-3.44 (m, 1H), 3.44-3.56 (m, 1H), 4.84 (s, 1H), 5.08 (d, *J* = 6.0 Hz, 1H), 6.64 (d, *J* = 8.2 Hz, 1H), 6.72 (d, *J* = 8.2 Hz, 1H), 7.12 (d, *J* = 7.9 Hz, 2H), 7.50 (d, *J* = 8.0 Hz, 2H), 7.53-7.61 (m, 3H), 7.96 (dd, *J* = 1.7, 7.8 Hz, 2H), 8.73 (s, 1H), 8.73 (s (broad), 1H), 9.56 (s (broad), 1H) ppm. ^{13}C NMR (75 MHz, DMSO-d_6) δ 20.66, 23.05, 24.63, 25.59, 25.61, 27.05, 27.18, 34.44, 45.83, 48.28, 51.77, 56.80, 57.11, 79.65, 87.89, 118.30, 120.08, 120.42, 125.37 (2C), 126.03, 126.77, 126.82, 127.96 (2C), 129.15, 131.46, 137.59, 140.09, 143.25, 145.46, 153.39, 167.41, 183.11, 206.02 ppm.

ACKNOWLEDGEMENTS

We are grateful to Dr. Sandro Neuner for his support on NMR measurements.

REFERENCES AND NOTES

1. V. Brower, *Lancet Oncol.*, 2017, **18**, e306; A. Markham, *Drugs*, 2017, **77**, 923; M. Inagaki, M. Kume, Y. Tamura, S. Hara, Y. Goto, N. Haga, T. Hasegawa, T. Nakamura, K. Koike, S. Oonishi, T. Kanemasa, and H. Kai, *Bioorg. Med. Chem. Lett.*, 2019, **29**, 73; A. Markham, *Drugs*, 2017, **77**, 923; H. Fujii, N. Hirano, H. Uchiro, K. Kawamura, and H. Nagase, *Chem. Pharm. Bull.*, 2004, **52**, 747.
2. M. Inagaki, S. Hara, N. Haga, Y. Tamura, Y. Goto, and T. Hasegawa, US 8084460, 2011.
3. Y. Tamura, K. Noguchi, M. Inagaki, K. Morimoto, N. Haga, S. Oda, and S. Omura, US 9108975, 2015.
4. The reaction was performed on 50-100 g scale.
5. Many reagents that are used for carbamate formation are quite harsh and/or generate salts on quenching with water, see reference 6.
6. F. Zafar and E. Sharmin, 2012, Polyurethane,' ed. by F. Zafar and E. Sharmin, IntechOpen, London, 2012, pp. 1-16.

7. C. Stock and R. Brückner, *Synlett*, 2010, 2429 (Mo-catalyst); H. Schäfer, A. Eichfelder, B. Gaspar, and Th. Pauen, WO 2014106578, 2014.
8. Ł. Górecki, A. Mucha, and P. Kafarski, *Beilstein J. Org. Chem.*, 2014, **10**, 883.
9. A. L. Spek, *Acta Cryst.*, 2009, **D65**, 148.
10. C. F. Macrae, I. J. Bruno, J. A. Chisholm, P. R. Edgington, P. McCabe, E. Pidcock, L. Rodriguez-Monge, R. Taylor, J. van de Streek, and P. A. Wood, *J. Appl. Cryst.*, 2008, **41**, 466.
11. T. Gelbrich and M. B. Hursthouse, *CrystEngComm*, 2005, **7**, 324.
12. T. Gelbrich, T. L. Threlfall, and M. B. Hursthouse, *CrystEngComm*, 2012, **14**, 5454.
13. G. M. Sheldrick, *SADABS. Version 2007/7*, 2007 Bruker AXS Inc., Madison, Wisconsin, USA.
14. G. M. Sheldrick, *Acta Cryst.*, 2015, **A71**, 3.
15. G. M. Sheldrick, *Acta Cryst.*, 2015, **C71**, 3.